

Article

Analysis of Re-Tensioning Time of Anchor Cable Based on New Prestress Loss Model

Keyou Shi ^{1,*} , Xiaoping Wu ^{1,2}, Yurong Tian ¹ and Xiaotian Xie ¹

¹ School of Civil Engineering, Central South University, Changsha 410075, China; xpwu@csu.edu.cn (X.W.); yurongtian@csu.edu.cn (Y.T.); xiaotian1997@csu.edu.cn (X.X.)

² National Engineering Laboratory for High Speed Railway Construction, Changsha 410075, China

* Correspondence: mucencia@csu.edu.cn

Abstract: Considering the interaction among anchor cable, frame beam and rock mass, a new model of prestress loss of anchor cable was established. The accuracy and applicability of the new model were verified by comparing the field monitoring data and the calculation results of existing models. In addition, based on the new model, the effect of the re-tension of the anchor cable at different time nodes was analyzed, and the later compensation time of anchor cable prestress was discussed. The research shows that: the accuracy of the new model is higher after considering the effect of the frame beam, the new model can not only calculate the loss of prestress of anchor cable, but also accurately predict the time when the prestress of anchor cable reaches the stable stage. The ideal effect of prestress compensation can be achieved when the anchor cable is re-tensioned at each time point after 20 days of the construction completed. The original prestress loss of the anchor cable is different, and the re-tension effect is also different, the greater the loss of the original prestress of the anchor cable, the more obvious the prestress compensation effect during the re-tension.



Citation: Shi, K.; Wu, X.; Tian, Y.; Xie, X. Analysis of Re-Tensioning Time of Anchor Cable Based on New Prestress Loss Model. *Mathematics* **2021**, *9*, 1094. <https://doi.org/10.3390/math9101094>

Academic Editor: José A. Tenreiro Machado

Received: 15 April 2021
Accepted: 7 May 2021
Published: 12 May 2021

Publisher's Note: MDPI stays neutral with regard to jurisdictional claims in published maps and institutional affiliations.



Copyright: © 2021 by the authors. Licensee MDPI, Basel, Switzerland. This article is an open access article distributed under the terms and conditions of the Creative Commons Attribution (CC BY) license (<https://creativecommons.org/licenses/by/4.0/>).

Keywords: prestress of anchor cable; creep model of rock mass; prestress loss model; prestress compensation; prestress loss

1. Introduction

During the construction of highways and railways, slope excavation will not only change the original stress state of a slope, but also accelerate the weathering speed of new exposed rock mass [1–4]; therefore, it is necessary to support the excavated slope along the road to improve the stability of the excavated slope, so as to ensure the operation safety of the road. There are many kinds of slope support methods, commonly used slope support structures include retaining wall [5–7], anti-slide pile [8,9], prestressed anchor rod [10,11] and prestressed anchor cable [12,13], among them, the prestressed anchor cable has been widely used in slope support engineering due to its advantages of reliable strength, simple construction and economic benefits. The prestressed anchor cable can fully exert its high strength through tensioning and to connect the weak structural plane of the rock mass with the stable rock stratum, so as to change the original stress state of the rock mass and improve the overall stability of the slope.

When prestressed anchor cables are used to reinforce the slope, the effective prestress of the anchor cables is the prerequisite guarantee for the anchor cables to play a supporting role. However, after long-term monitoring of the prestress of anchor cables of the slope, many studies have found that the loss of anchor cable prestress is very common in anchored engineering [14–17]. In addition, some studies have established some physical models [18–21] and expounded the phenomenon of prestress loss of anchor cable in multiple directions through theoretical analysis. These models generally believe that the long-term loss of anchor cable prestress is mainly related to the creep of reinforced rock mass, under the long-term action of the tensioning load of the anchor cable, creep deformation occurs in rock mass, which causes the rebound shrinkage of anchor cable,

and then causes the long-term loss of anchor cable prestress. However, these models only build physical models of anchor cable and rock mass, and ignore the role of frame beam in anchored slope, the establishment of the prestress loss model of anchor cable is based on the assumption that the rock mass is uniformly stressed and the frame beam is the guarantee of uniform stress of rock mass in anchored slope, therefore, the role of frame beam should not be ignored in the physical modeling of prestress loss of anchor cable.

In addition, because the prestress loss of anchor cables directly affects the supporting effect of slope, in actual projects, after the completion of construction, most of them will use the method of re-tensioning to compensate the prestress of anchor cable. The re-tensioning time of the anchor cable has a direct impact on its prestress compensation effect, clarifying the re-tensioning time of the anchor cable can not only ensure the effect of prestress compensation, but also facilitate the scheduling of on-site personnel and the overall arrangement of construction. The remainder of this paper is organized as follows: in Section 2, the new prestress loss model of anchor cable considering the action of frame beam was established, in Section 3, the on-site monitoring test was carried out and the accuracy of the new model were verified by comparing the on-site monitoring data and the calculation results of existing models, in Section 4, the effect of the re-tension of the anchor cable at different time nodes was analyzed. The main conclusions are summarized in Section 5.

2. Prestress Loss Model of Anchor Cable Considering the Action of Frame Beam

The long-term prestress loss of anchor cable is mainly determined by the material properties of anchor cable itself and the mechanical properties of rock mass, therefore, the calculation model of prestress loss of anchor cable is generally established by reasonably combining the calculation model of anchor cable and rock mass [22–25], as we all know, the premise of establishing the coupled creep model is to assume that the rock mass is uniformly stressed [19,26], from the previous analysis, it can be seen that the frame beam is the guarantee of the uniform stress of the rock mass, and the actual stress of the rock mass under the action of the frame beam can be closer to the assumed condition, Therefore, the role of frame beam should not be ignored in the establishment of prestress loss model of anchor cable.

2.1. Analysis Model of Anchor Cable

In actual engineering, the deformation of anchor cable in anchored slope under service condition is mainly elastic deformation, so the Hooke model in Figure 1 can be used to simulate the anchor cable. The constitutive relationship of the model is:

$$\varepsilon = \frac{\sigma}{E_C} \quad (1)$$

where ε is the strain of the anchor cable body within the anchorage range; σ is the stress of the anchor cable body within the anchorage range; E_C is the equivalent elastic modulus of the anchor cable body within the anchorage range.

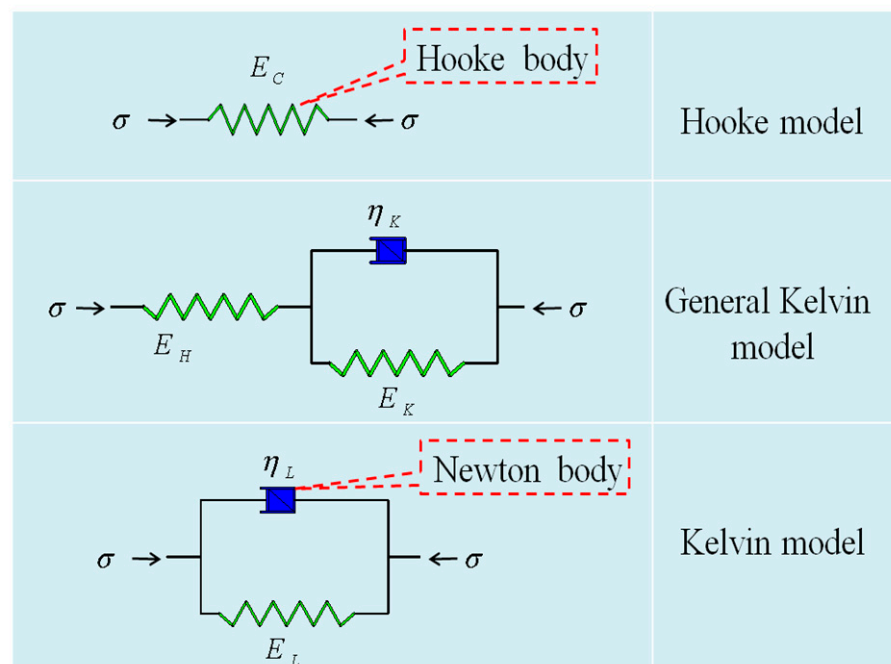


Figure 1. Analysis model of each part.

2.2. Analysis Model of Rock Mass

Under the action of stress, the rock mass not only has the characteristics of instantaneous stress relaxation and elastic deformation, but also has the characteristics of viscoelastic plasticity under the action of long-term stress. Therefore, the General Kelvin model in Figure 1 can be used to simulate the rock mass. The General Kelvin model is developed on the basis of Kelvin model, which describes the various stages of rock mass creep. The constitutive relationship of the model is:

$$\frac{\eta_K}{E_H + E_K} \sigma' + \sigma = \frac{\eta_K E_H}{E_H + E_K} \epsilon' + \frac{E_H E_K}{E_H + E_K} \epsilon \tag{2}$$

where η_K is the viscous coefficient of the rock mass; E_K is the viscoelastic modulus of the rock mass; E_H is the instantaneous elastic modulus of the rock mass; σ' is the first derivative of the stress; ϵ' is the first derivative of the strain.

2.3. Analysis Model of Frame Beam

Compared with rock mass, the frame beam is a reinforced concrete structure with high stiffness, and the section size of the frame beam is far less than the thickness of the rock layer, so the instantaneous elastic strain of the frame beam can be ignored under the stress, therefore, the Kelvin model in Figure 1 can be used to simulate the frame beam, and the constitutive relationship of the model is:

$$\sigma = \eta_L \epsilon' + E_L \epsilon \tag{3}$$

where η_L is the viscous coefficient of the frame beam; E_L is the viscoelastic modulus of the frame beam.

2.4. Establishment of Prestress Loss Model of Anchor Cable

The interaction relationship among the anchor cable, frame beam and rock mass is shown in Figure 2. In the actual construction process, the anchor cable is installed in the borehole, and then the anchor cable structure is combined with the rock mass by grouting into the borehole. Therefore, it can be considered that the retraction deformation of the anchor cable and the creep deformation of the rock mass are carried out simultaneously.

Since there is no grout bond between the anchor cable structure and the frame beam, it can be considered that the retraction deformation of the anchor cable and the creep deformation of the frame beam are relatively independent.

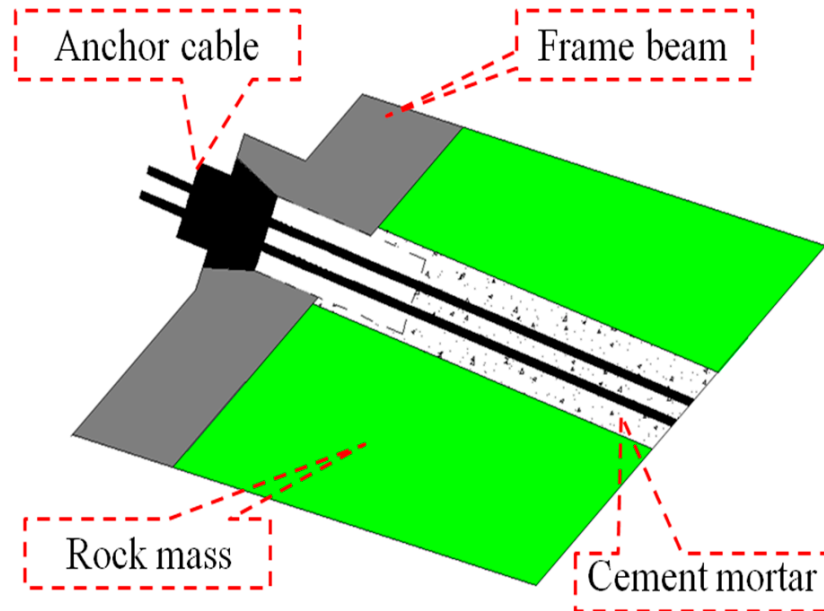


Figure 2. Schematic diagram of slope supported by anchor cables and frame beam.

Therefore, combined with the position of anchor cable, frame beam and rock mass in Figure 2 and the interaction relationship among them, the prestress loss model of anchor cable as shown in Figure 3 is established. The model is established by connecting Part 1 and Part 2 in parallel, and then connecting Part 3 in series, in the model, Part 1 is a General Kelvin model, which is used to simulate rock mass; Part 2 is Hooke model, which is used to simulate anchor cable; Part 3 is Kelvin model, which is used to simulate frame beam.

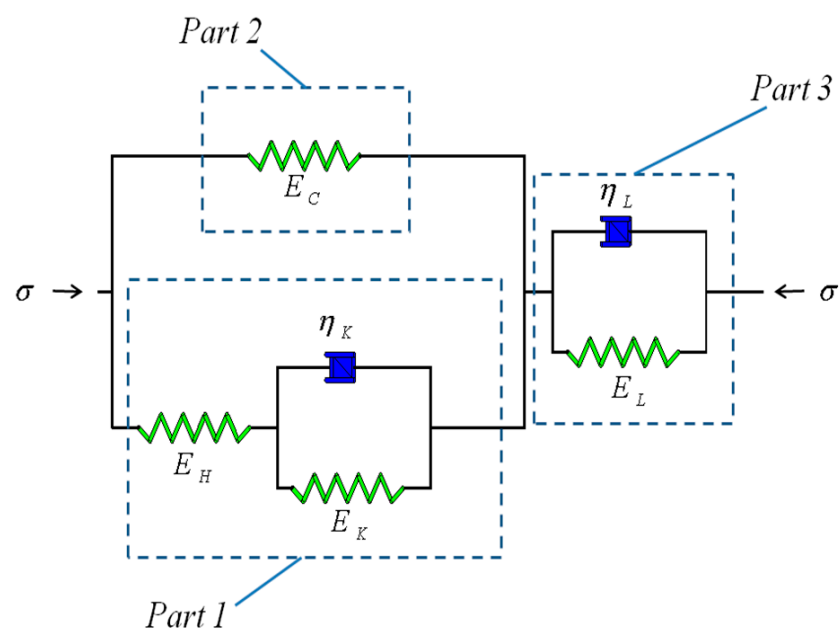


Figure 3. New prestress loss model of anchor cable.

2.5. Derivation of Model Calculation Formula

According to the prestress loss model of anchor cable shown in Figure 3, the stress-strain relationship among anchor cable, frame beam and rock mass should meet the following equation:

$$\sigma = \sigma_L = \sigma_N + \sigma_C \quad (4)$$

$$\varepsilon = \varepsilon_L + \varepsilon_N = \varepsilon_L + \varepsilon_C \quad (5)$$

where σ is the total stress of prestress loss model; ε is the total strain of prestress loss model; σ_L and ε_L are the stress and strain of frame beam; σ_N and ε_N are the stress and strain of rock mass; σ_C and ε_C are the stress and strain of anchor cable body.

The following equation can be obtained by transforming Equations (4) and (5):

$$\sigma_N = \sigma - \sigma_C = \sigma - (\varepsilon - \varepsilon_L)E_C = \frac{(E_C + E_L)\sigma}{E_L} - \varepsilon E_C \quad (6)$$

$$\varepsilon_N = \varepsilon - \varepsilon_L = \varepsilon - \frac{\sigma}{E_L} \quad (7)$$

By substituting Equations (6) and (7) into Equation (3), the constitutive equation of the established prestress loss calculation model can be obtained:

$$\sigma' + A\sigma = B\varepsilon' + C\varepsilon \quad (8)$$

$$A = \frac{(E_C + E_L)(E_H + E_K) + E_H E_K}{\eta_K E_C + \eta_K E_L + \eta_K E_H} \quad (9)$$

$$B = \frac{E_H E_L + E_C E_L}{E_C + E_L + E_H} \quad (10)$$

$$C = \frac{E_H E_K E_L + E_C E_L (E_H + E_K)}{\eta_K E_C + \eta_K E_L + \eta_K E_H} \quad (11)$$

At the initial moment of prestress loss of anchor cable (i.e., $t = 0$), assuming that the initial stress and initial strain of prestress loss model are σ_0 and ε_0 respectively, Equation (8) can be transformed into the stress relaxation equation of prestress loss model:

$$\sigma' + A\sigma = C\varepsilon_0 \quad (12)$$

The solution of differential Equation (12) can be obtained as follows:

$$\sigma = C_1 \exp(-At) + \frac{C\varepsilon_0}{A} \quad (13)$$

When the stress is applied on the rock mass at the beginning, it can be considered that the deformation of rock mass is mainly elastic deformation, so the initial strain of the model is $\varepsilon_0 = \sigma_0 / (E_C + E_H) + \sigma_0 / E_L$. When considering the initial condition $\sigma = \sigma_0$ ($t = 0$), and combining with Equation (12), the value of coefficient C_1 can be obtained:

$$C_1 = \sigma_0 - \frac{C}{A}\varepsilon_0 \quad (14)$$

Through the above equations, the loss of prestress can be calculated and analyzed under the condition that the initial strain ε_0 is known.

3. Model Validation Based on On-Site Monitoring Data

3.1. On-Site Monitoring Test

The EK1 + 555–EK1 + 706.93 section of the Zhengxi (Zhengzhou to Xixia) highway is located in Miaozi Town, Luoyang City, China. This area is marked by canyons, with dangerous and undulating terrain, and there are a large number of deep excavation slopes.

The upper part of the slope is covered by Quaternary residual slope deposit with a small thickness. The lower layer of rock and soil mass is divided into two geological engineering layers: strongly weathered quartz schist and fully weathered quartz schist. The excavation depth of the slope is mainly composed of fully weathered quartz schist. The groundwater in this deep cutting section is mainly Quaternary loose rock fissure water and bedrock fissure water, and the recharge source is meteoric water and surface river water infiltration. No groundwater level is found during the survey. The on-site monitoring in this study is based on the deep cutting slope in the EK1 + 640 section. The maximum excavation depth of the slope is 70.6 m, and the monitoring slope is divided into seven stages for excavation. The reinforcement scheme of the slope is shown in Figure 4. The fourth and fifth level slopes are supported by frame beam and prestressed anchor cables. The length of anchor cable is 22 m, the length of anchorage section is 10 m, the vertical spacing between anchor cables is 2 m, the angle between anchor cable and horizontal direction is 20° and the actual tension load of anchor cable is 380 kN/m. The diameter of anchor hole is 130 mm, and M40 cement mortar is used for grouting. Each anchor cable is composed of four steel strands. The diameter of the steel strand is 15 mm, the nominal area is 140 mm^2 , the tensile strength σ_T is 1860 MPa, and the elastic modulus E is $1.95 \times 10^5 \text{ MPa}$. The frame beam is poured using C25 concrete. The interface dimensions of the frame beam are $0.4 \times 0.4 \text{ m}^2$, and the elastic modulus E_L is $2.8 \times 10^4 \text{ MPa}$.

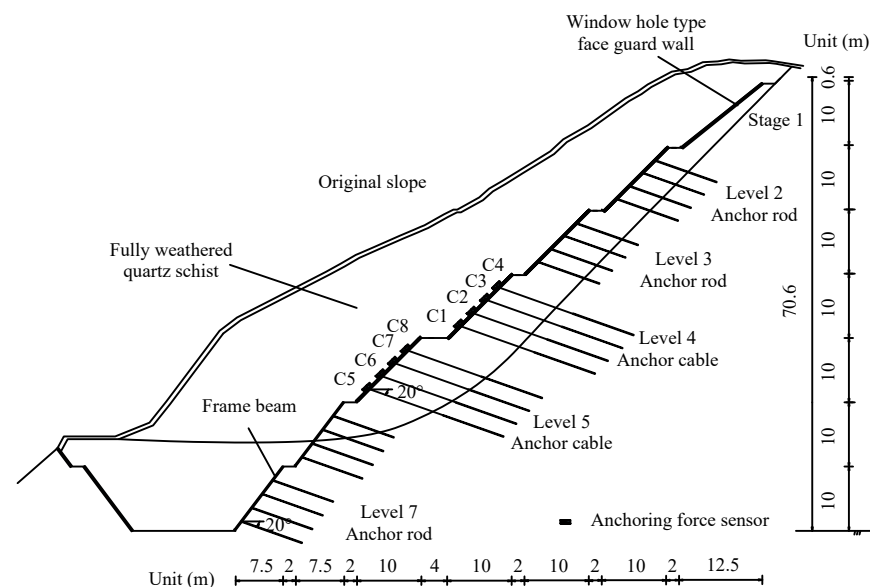


Figure 4. Reinforcement scheme of EK1 + 640 deep cutting slope.

Before the eight anchor cables of the fourth and fifth level slopes were tensioned, an anchoring force sensor was installed. The monitoring data acquisition methods are as follows: (1) installation of the DSC (data-operation supervise center) wireless data acquisition system on site; (2) using the internet function of the GPRS (general packet radio service), establish a live internet mobile phone module by agreeing on the domain name; (3) receive data through the wireless network using a computer with professional software installed.

Figure 5 shows the monitoring curves of the prestress of anchor cables of the fourth and fifth level slopes. It can be seen that, unlike the axial force growth of the anchor rod, the prestress of all the anchor cables will lose to different degrees after the anchor cable tension is completed. This is because under the action of anchoring load, the cracks in the rock mass are further compressed, resulting in compression deformation, which leads to the stress relaxation of the anchor cable. Although the upper completely weathered layer slides along the rock interface during the excavation of the lower slope, resulting in lateral deformation, it will play a certain role in the tension of the anchor cable. However, the

design length of the anchor cable is 22 m, which is closely connected with the deep rock mass of the cutting slope. The compression deformation of the crack at the deep weathered rock mass is greater than the lateral deformation of the slope, which makes the prestress of the anchor cables lose in different degrees. It can be seen that, compared with the anchor rod, the action length of the anchor cable is longer and its stress is more complex. The prestress of the anchor cable is not only related to the lateral deformation of the slope, but also related to the deformation of the anchorage, the shrinkage of the steel strand, the compaction of the cracks in the weathered rock mass and the creep deformation of the rock mass.

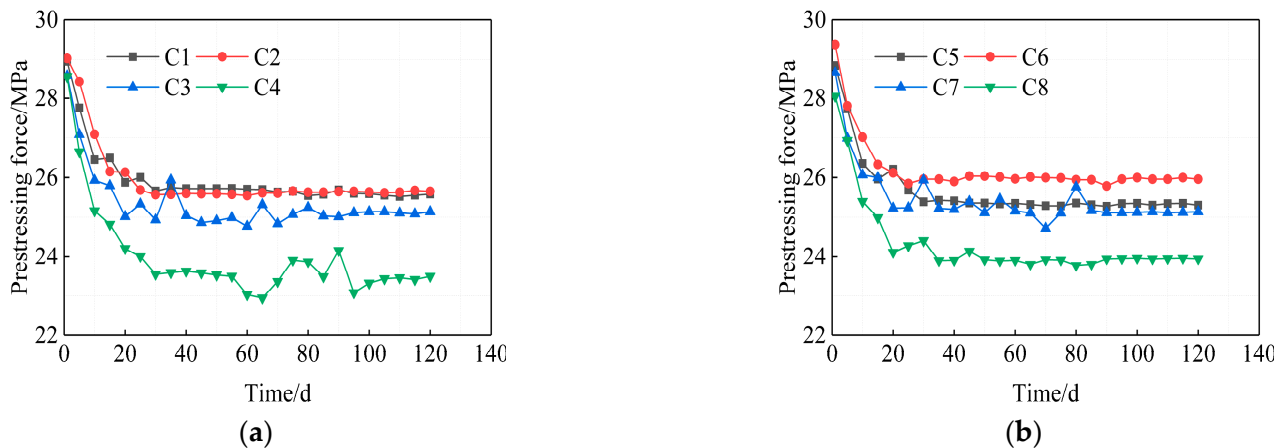


Figure 5. Monitoring curves of the prestress of the anchor cables: (a) the anchor cables of the fourth level slope; (b) the anchor cables of the fifth level slope.

Further analysis of the monitoring results shows that the prestress loss of anchor cable C4 and anchor cable C8 is the largest. Combined with the acting position of each anchor cable in Figure 4, it can be seen that the anchor cable with larger prestress loss is concentrated acting on top of each stage slope. In addition, we can also see that the prestress of the anchor cables acting on top of each level slope also has obvious fluctuation phenomenon, which indicates that they are greatly affected by environmental changes and construction disturbance. It can be seen that for the slope strengthened by multi anchor cables, the variation of prestress of anchor cables at different positions is quite different, which can easily lead to uneven stress of frame beam, resulting in large tensile stress of frame beam, and then cracking of concrete, therefore, during construction, the construction technology should be improved as much as possible, the flatness and tensioning technology of the frame beam at the anchor installation place should be improved, and the flatness and tension technology of the frame beam at the anchorage installation site should be improved as much as possible, so as to reduce the unbalanced prestress loss of slope reinforced by multiple anchor cables.

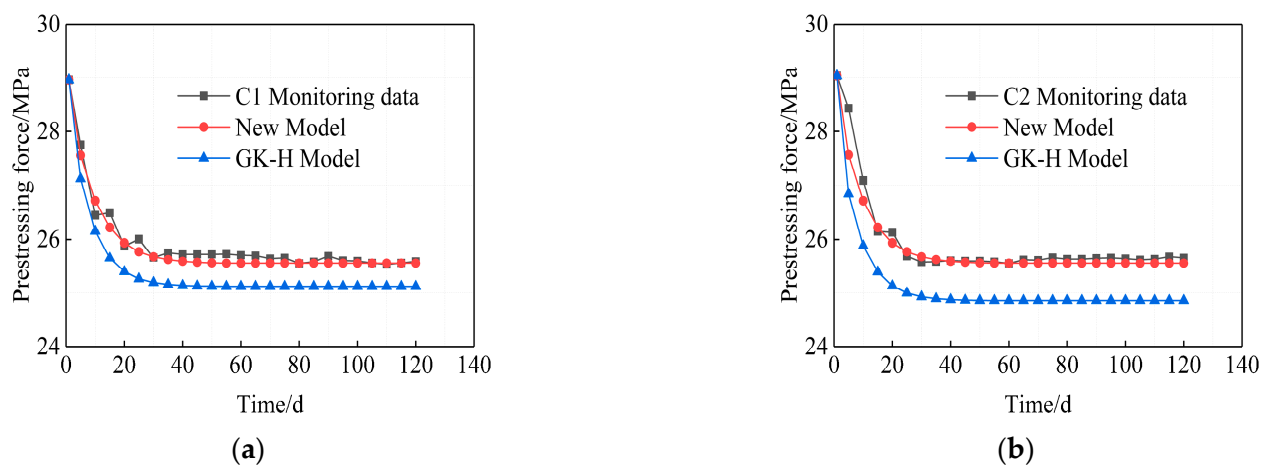
3.2. Model Validation

Combined with the construction of the supporting project (Zheng-xi highway), the prestress monitoring of anchor cables was carried out on the deep cutting slopes of EK1+640 section, at the same time, the corresponding field creep test of rock mass was carried out. Here, the prestress monitoring results of two anchor cables (cable C1 and C2) are taken to verify the model. Table 1 shows the calculation parameters of the model, in which E_C is converted from the actual parameters of the steel strand used in the project, E_L is the actual parameters of C25 concrete used in the frame beam, and E_H , E_K and η_K are obtained by parameter inversion combined with the field creep test results of the rock mass.

Table 1. Model calculation parameters.

E_C /GPa	E_L /GPa	E_H /GPa	E_K /GPa	η_K /GPa.day
8.23	28	41.91	57.5	597

The model in this paper is established based on the existing model by adding frame beam elements. In order to further verify the accuracy of the model, in addition to the field monitoring data, the calculation results of GK-H model [18] are added in Figure 6 for comparative analysis. As shown in the monitoring data in Figure 6, the prestress of each anchor cable will have different degrees of loss after the construction. In the initial stage of monitoring, the prestress loss rate of anchor cable is the fastest, and the proportion of prestress loss is also the largest. In the later stage of monitoring, the change of prestress of anchor cable tends to be slow. In addition, due to the influence of construction disturbances such as slope excavation, the prestress of anchor cable of slope will fluctuate in actual engineering. According to the model calculation curves (New model, GK-H model) in Figure 6, it can be seen that in view of the limitations of theoretical analysis, the model calculation curves are the smoothly changing curves, and they cannot reflect the fluctuation of anchor cable prestress.

**Figure 6.** Model validation: (a) cable C1; (b) cable C2.

However, from the point of view of model verification alone, except that the fluctuation of anchor cable prestress cannot be reflected, the calculation results of the new model in this paper are almost the same as the trends of field monitoring results. The GK-H model only considers the coupled effect of anchor cable and rock mass (*Part 1* and *Part 2* in Figure 3), but does not consider the role of frame beam in the anchored structure, resulting in the calculation results of GK-H model is lower than the field monitoring results. Therefore, in a comprehensive comparison, the accuracy of the new model is higher after considering the effect of the frame beam, the new model can not only calculate the loss of prestress of anchor cable, but also accurately predict the time when the prestress of anchor cable reaches the stable stage.

4. Re-Tensioning Time of Anchor Cable Prestress

In the slope anchorage engineering, different degrees of prestress loss will occur after the anchor cable tensioning is completed, after the construction is completed for a period of time, the re-tensioning of anchor cable can effectively compensate for the prestress loss caused by rock creep, the re-tensioning time of anchor cable directly affects the effect of prestress compensation of anchor cable, so it is of great engineering significance to study the compensation time of prestress of anchor cable.

According to the previous analysis, Equation (13) can be used to calculate the prestress of the anchor cable under the condition that the initial strain ϵ_0 is known. When the anchor cable is re-tensioned at time t after the completion of construction, the initial condition (initial strain) of the model in Figure 3 has changed, and the changed initial strain is as follows:

$$\epsilon_0' = \epsilon_0 + \frac{\bar{\sigma} - \sigma_t}{E_C + E_H} + \frac{\bar{\sigma} - \sigma_t}{E_L} \tag{15}$$

$$\bar{\sigma} = \frac{T}{A_C} \tag{16}$$

where ϵ_0' is the initial strain corresponding to time t ; σ_t is the total stress of the loss model at time t ; $\bar{\sigma}$ is the total stress of the loss model after re-tensioning; T is the predetermined re-tensioning load of the anchor cable; A_C is the equivalent sectional area of the anchor cable body.

The analysis is also carried out with the four anchor cables (cable C1 to C4) of deep cutting slope of EK1 + 640 section of Zheng-Xi highway as the background, it can be seen from Figure 6 that the time for the prestress of each anchor cable to stabilize is about 30 days, therefore, the time points $t = 5, t = 10, t = 20$ and $t = 30$ after the completion of construction can be taken as the time points for the re-tensioning calculation of the anchor cables, and the prestress compensation effect of each anchor cable under each time point can be discussed.

The variation curves of prestress of anchor cables at different compensation time are shown in Figure 7. It can be seen that although there is still prestress loss in each anchor cable after re-tensioning, the prestress loss of each anchor cable after re-tensioning is less than its original loss, and the later the re-tensioning time is, the smaller the prestress loss of each anchor cable is, the reason is that the long-term prestress loss of the anchor cable is related to the creep of each part of the anchor body. The longer the action time of the anchor cable is, the smaller the creep of each part of the anchor body is. Therefore, when the re-tensioning time is later, the prestress loss of each anchor cable is smaller.

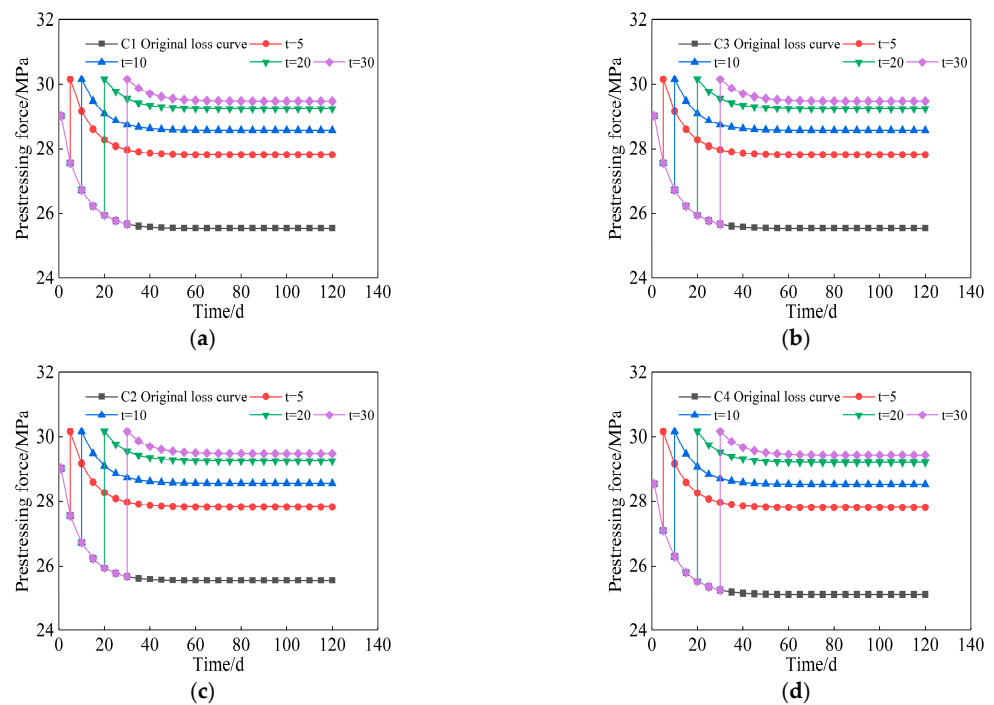


Figure 7. Variation curves of prestress force of each anchor cable at different re-tensioning time: (a) cable C1; (b) cable C2; (c) cable C3; (d) cable C4.

In addition, by analyzing the single anchor cable separately (e.g., cable C1), after the re-tensioning of anchor cable C1 on times $t = 5$, $t = 10$, $t = 20$ and $t = 30$, the prestress values when it tends to be stable are 27.76, 28.50, 29.18 and 29.41 MPa respectively, and the differences between the two are 0.74, 0.68 and 0.23 MPa respectively. It can be seen that, although theoretically speaking, the later the re-tensioning time is, the greater the stable value of prestress after the re-tensioning of anchor cable is, however, the difference of the stable value of prestress after the re-tensioning of anchor cable C1 at times $t = 20$ and $t = 30$ is not very large. Therefore, the ideal effect of prestress compensation all can be achieved when the anchor cable is re-tensioned at each time point after 20 days of the construction completed.

In the multi-anchor supporting slope, the loss of prestress of each anchor cable is not the same, when the anchor cables with different prestress loss are re-tensioned, the effect of prestress compensation will also be different. In this paper, the concept of prestress compensation ratio (the ratio of the stable prestress value of the anchor cable after re-tensioning to its original stable prestress value) is introduced. Table 2 shows the stable value of prestress of each anchor cable at different re-tensioning time. Taking the results of day $t = 30$ as an example, the original prestress stable values of anchor cables C1 to C4 are 25.55, 25.75, 25.16 and 25.13 MPa, respectively, the smaller the stable value is, the greater the prestress loss is. When the anchor cables C1 to C4 are re-tensioned in day $t = 30$, the stable value of prestress of anchor cables C1 to C4 are 29.41, 29.48, 29.44 and 29.43 MPa respectively, and the prestress compensation ratios are 1.151, 1.144, 1.170 and 1.171 respectively. It can be seen that the greater the original loss of the anchor cable is, the greater the prestress compensation ratio is, which means the better the prestress compensation effect is.

Table 2. Stable value of prestress force of each anchor cable at different re-tensioning time.

Anchor Cable Number	Time t/d	Stable Value of Original Anchor Cable Prestress σ_t /MPa	Stable Value of Anchor Cable Prestress after Re-tensioning σ /MPa	Prestress Compensation Ratio
C1	5	25.55	27.76	1.086
	10	25.55	28.50	1.115
	20	25.55	29.18	1.142
	30	25.55	29.41	1.151
C2	5	25.75	27.82	1.080
	10	25.75	28.57	1.110
	20	25.75	29.25	1.136
	30	25.75	29.48	1.144
C3	5	25.16	27.80	1.105
	10	25.16	28.54	1.134
	20	25.16	29.21	1.161
C4	30	25.16	29.44	1.170
	5	25.13	27.81	1.107
	10	25.13	28.53	1.135
	20	25.13	29.21	1.162
	30	25.13	29.43	1.171

5. Conclusions

- (1) The frame beam is the guarantee for the uniform stress of the rock mass of the anchored slope, and the role of the frame beam should not be ignored in the stress analysis of the anchored slope, in view of the interaction among the anchor cable, the frame beam and the rock mass, the new prestress loss model of the anchor cable is established, and compared with the field monitoring data and existing model, the accuracy of the new model is verified.
- (2) Based on the new established prestress loss model of the anchor cable, the prestress compensation time of anchor cable is studied. Although theoretically speaking, the

later the re-tensioning time is, the greater the stable value of prestress after the re-tensioning of anchor cable is, however, there is little difference in the stable value of prestress when the anchor cable is re-tensioned at each time point after 20 days of the construction completed. It can be considered that the ideal effect of prestress compensation all can be achieved when the anchor cable is re-tensioned at each time point after 20 days of the construction completed.

- (3) In the multi-anchor supporting slope, the loss of prestress of each anchor cable is not the same, when the anchor cables with different prestress loss are re-tensioned, the effect of prestress compensation will also be different. The greater the original loss of the anchor cable is, the greater the prestress compensation ratio is, which means the better the prestress compensation effect is.

Author Contributions: Conceptualization, K.S. and X.W.; methodology, K.S.; software, Y.T.; validation, K.S., X.X. and Y.T.; formal analysis, Y.T.; investigation, X.X.; resources, K.S.; data curation, Y.T.; writing—original draft preparation, K.S.; writing—review and editing, X.W.; visualization, K.S.; supervision, X.W.; project administration, X.W.; funding acquisition, X.W. All authors have read and agreed to the published version of the manuscript.

Funding: This research was funded by Hunan Provincial Department of Transportation Foundation of China (No. 201901).

Institutional Review Board Statement: Not applicable.

Informed Consent Statement: Not applicable.

Data Availability Statement: Not applicable.

Conflicts of Interest: The authors declare no conflict of interest.

References

1. Ersoz, T.; Topal, T. Assessment of rock slope stability with the effects of weathering and excavation by comparing deterministic methods and slope stability probability classification (SSPC). *Environ. Earth Sci.* **2018**, *77*. [[CrossRef](#)]
2. Li, Q.; Wang, Y.M.; Zhang, K.B.; Yu, H.; Tao, Z.Y. Field investigation and numerical study of a siltstone slope instability induced by excavation and rainfall. *Landslides* **2020**, *17*, 1485–1499. [[CrossRef](#)]
3. Ma, K.; Xu, N.W.; Liang, Z.Z. Stability Assessment of the Excavated Rock Slope at the Dagangshan Hydropower Station in China Based on Microseismic Monitoring. *Adv. Civ. Eng.* **2018**, *2018*. [[CrossRef](#)]
4. Najib, N.; Fukuda, D.; Kodama, J.-I.; Fujii, Y. The Deformation Modes of Rock Slopes due to Excavation in Mountain-Type Mines. *Mater. Trans.* **2015**, *56*, 1159–1168. [[CrossRef](#)]
5. Xu, P.; Hatami, K.; Bao, J.J.; Li, T. Bearing capacity and failure mechanisms of two-tiered reinforced soil retaining walls under footing load. *Comput. Geotech.* **2020**, *128*, 17. [[CrossRef](#)]
6. Wang, X.; Shrestha, R.; Li, X.; Mandal, A.K. Design Theory and Method of Geo-Synthetic Reinforced Soil Retaining Wall Combined with a Gravity Retaining Wall or Full Height Rigid Facing. *Geotech. Geol. Eng.* **2021**, *39*, 2075–2086. [[CrossRef](#)]
7. Munoz-Medina, B.; Ordonez, J.; Romana, M.G.; Lara-Galera, A. Typology Selection of Retaining Walls Based on Multicriteria Decision-Making Methods. *Appl. Sci.* **2021**, *11*, 1457. [[CrossRef](#)]
8. Chen, H.; Zhang, G.; Chang, Z.; Wen, L.; Gao, W. Failure Analysis of a Highway Cut Slope with Anti-Slide Piles. *Geofluids* **2021**, *2021*. [[CrossRef](#)]
9. Zhang, J.W.; Wang, X.J.; Wang, H.; Qin, H.Y. Model Test and Numerical Simulation of Single Pile Response under Combined Loading in Slope. *Appl. Sci.* **2020**, *10*, 6140. [[CrossRef](#)]
10. Yuan, C.; Fan, L.; Cui, J.F.; Wang, W.J. Numerical Simulation of the Supporting Effect of Anchor Rods on Layered and Nonlayered Roof Rocks. *Adv. Civ. Eng.* **2020**, *2020*, 14. [[CrossRef](#)]
11. Puccinelli, M. Considerations on the bond strength value in the anchor rods design. *Gallerie Gd. OpereSotter.* **2018**, *127*, 29–35.
12. An, C.-L.; Liang, Y.; Wang, L.-Q.; Deng, S.; Sun, Z.-H.; Fan, B.-Q.; Zheng, L.-B. Three-dimensional optimization design for the direction angle of anchor cable reinforcement in wedge rock slope. *Rock Soil Mech.* **2020**, *41*, 2765–2772. [[CrossRef](#)]
13. Li, J.; Chen, S.X.; Yu, F.; Jiang, L.F.; Dai, Z.J. Discussion on mechanism of reinforcing high and steep slope with prestressed anchor cable. *Rock Soil Mech.* **2020**, *41*, 707–713. [[CrossRef](#)]
14. Fan, Q.; Zhu, H.; Geng, J. Monitoring result analyses of high slope of five-step ship lock in the Three Gorges Project. *J. Rock Mech. Geotech. Eng.* **2015**, *7*, 199–206. [[CrossRef](#)]
15. Sung, H.-J.; Tan Manh, D.; Kim, J.-M.; Kim, Y.-S. Long-term monitoring of ground anchor tensile forces by FBG sensors embedded tendon. *Smart Struct. Syst.* **2017**, *19*, 269–277. [[CrossRef](#)]

16. Kim, Y.-S.; Sung, H.-J.; Kim, H.-W.; Kim, J.-M. Monitoring of tension force and load transfer of ground anchor by using optical FBG sensors embedded tendon. *Smart Struct. Syst.* **2011**, *7*, 303–317. [[CrossRef](#)]
17. Lu, G.R.; Wang, Q.B.; Li, X.; Wang, L. Study and Practice of Controlling Anchorage Force Loss of Prestressed Anchor Rope. *Appl Mech Mater.* **2012**, *166–169*, 1663–1668. [[CrossRef](#)]
18. Wang, Q.B.; Zhang, C.; Wang, H. Study of coupling effect between anchorage force loss of prestressed anchor cable and rock and soil creep. *Rock Soil Mech.* **2014**, *35*, 2150–2156. (In Chinese) [[CrossRef](#)]
19. Chen, G.; Chen, T.; Chen, Y.; Huang, R.; Liu, M. A new method of predicting the prestress variations in anchored cables with excavation unloading destruction. *Eng. Geol.* **2018**, *241*, 109–120. [[CrossRef](#)]
20. Chen, T.; Chen, G.Q.; Huang, R.Q.; Liu, M. A model of anchorage force loss of anchor cable during high slope strong unloading. *Rock Soil Mech.* **2018**, *39*, 4125–4132. (In Chinese) [[CrossRef](#)]
21. Wang, G.F.; Qing, L.; Lu, L.; Cao, Z.; Wang, W. A Coupled Model Research of Anchor Prestress Loss Considering the Relaxation Characteristics of Anchor. *Chin. J. Undergr. Space Eng.* **2017**, *13*, 1585–1591. (In Chinese)
22. Trzeciak, M.; Sone, H.; Dabrowski, M. Long-term creep tests and viscoelastic constitutive modeling of lower Paleozoic shales from the Baltic Basin, N Poland. *Int. J. Rock Mech. Min. Sci.* **2018**, *112*, 139–157. [[CrossRef](#)]
23. Liu, H.Z.; Xie, H.Q.; He, J.D.; Xiao, M.L.; Zhuo, L. Nonlinear creep damage constitutive model for soft rocks. *Mech. Time-Depend. Mater.* **2017**, *21*, 73–96. [[CrossRef](#)]
24. Zhu, W.; Dai, G.; Gong, W. Study on Cyclic Cumulative Deformation Characteristics and the Equivalent Cyclic Creep Model of Soft Clay. *Math. Probl. Eng.* **2021**, *2021*. [[CrossRef](#)]
25. Zhang, Q.; Song, Z.; Wang, J.; Zhang, Y.; Wang, T. Creep Properties and Constitutive Model of Salt Rock. *Adv. Civ. Eng.* **2021**, *2021*. [[CrossRef](#)]
26. Shi, K.Y.; Wu, X.P.; Liu, Z.; Dai, S.L. Coupled calculation model for anchoring force loss in a slope reinforced by a frame beam and anchor cables. *Eng. Geol.* **2019**, *260*, 9. [[CrossRef](#)]